RESEARCH ARTICLE

Computed Tomographic Assessment of Liver in Dog Cadaver

Kaveri S. Sohoni, Vinod D. Shankhapal*, Santosh A. Gaikwad, Girish U. Yadav, Sanjay B. Lambate

Abstract

The present study was conducted to perform a detailed anatomical and imaging-based evaluation of liver in eight embalmed non-descript adult male dog cadavers. Helical non-contrast computed tomographic (CT) examination enabled cross-sectional visualization of liver in transverse, sagittal and dorsal planes and helped determine its spatial relationships and topographical position according to thoracic (T) and lumbar (L) vertebrae. The dog cadavers were procured and embalmed using Thiel's solution. Non-contrast helical CT imaging was performed using a 128-slice computed tomographic scanner with slice thickness of 0.6 mm, and reconstruction interval of 0.3 mm using soft tissue window settings (window width 350 HU; window level 40 HU). In CT examination, liver appeared as a homogeneous soft tissue structure occupying the cranial abdominal cavity, extending from eighth thoracic (T8) to first lumbar (L1) vertebral levels. The hepatic parenchyma appeared to be continuous with the diaphragm. The mean attenuation value of liver recorded in the present study was 68.68 ± 5.48 HU. Minor alteration in the tissue density of liver (54.2-89.0 HU) was observed, which may be due to embalming of dog cadaver. The liver was hyperattenuating to the muscle and hypoattenuating to the bony structures of the ribs, vertebrae or sternum. The liver was hyperattenuating than the falciform ligament, mesentery and the perirenal fat.

Key words: Computed tomography, Dog, Liver.

Ind J Vet Sci and Biotech (2026): 10.48165/ijvsbt.22.4.21

Introduction

Diagnostic imaging has become an essential tool in modern veterinary medicine, playing a critical role in diagnosing, treating, and managing animal health conditions. Computed tomography has been applied in the dog to evaluate various organs (Hoey *et al.,* 2012). It is able to scan and visualize large and fine anatomical structures in the body and yields easier, faster, and accurate diagnoses. In veterinary medicine although computed tomography is mostly used for diagnostic purposes in small animals, but in recent years computed tomography has also been used as a non-invasive modality in non-clinical studies. This advanced modality allows accurate evaluation of soft tissues, bones, and organs, enhancing the diagnosis and management of diseases. Liver disease is a common problem encountered in small animal practice. Many animals with liver disease manifest vague malaise, with variable clinical signs such as icterus, ascites, jaundice, weight loss, hyper salivation, coagulopathy, lethargy, anorexia, vomiting, and diarrhoea (Mannion, 2006). In veterinary medicine, x-ray and ultrasound are the imaging modalities of choice for the abdomen, although, it is increasingly recognized that computed tomography can provide information that cannot be obtained by other means (Gavrilas *et al.*, 2016). Computed tomography provides precise visualization of the liver parenchyma and associated organs like the gall bladder as well as surrounding structures and organs like falciform fat and stomach. In recent years, advanced imaging techniques have been successfully performed in animals. However, meagre information is available on computed tomographic assessment of liver in embalmed dog cadavers. Hence, the present research work was carried out for computed tomographic assessment of the liver of embalmed dog cadaver.

Department of Veterinary Anatomy and Histology, Mumbai Veterinary College, Mumbai, Parel-400012, Maharashtra Animal and Fishery Sciences University, Maharashtra, India

Corresponding Author: Dr. V. D. Shankhapal, Professor, Department of Veterinary Anatomy and Histology, Mumbai Veterinary College, Mumbai, Parel-400012, MAFSU, Maharashtra, India. e-mail: dr.vds@rediffmail.com

How to cite this article: Sohoni, K. S., Shankhapal, V. D., Gaikwad, S. A., Yadav, G. U., & Lambate, S. B. (2026). Computed Tomographic Assessment of Liver in Dog Cadaver. Ind J Vet Sci and Biotech, 22(4), 113-118.

Source of support: Nil

Conflict of interest: None

Submitted 23/04/2026 **Accepted** 21/05/2026 **Published** 10/07/2026

Materials and Methods

The present study was carried out on liver of eight non-descript, male, adult embalmed dog cadavers. The fresh cadavers were procured from the Bai Sakarabai Dinshaw Petit Hospital for Animals (BSDPHA), Parel, Mumbai. The clinical history of these dogs was collected to ensure that the cadavers were free from any liver pathology. The dog cadavers were embalmed using Thiel's embalming solution at the Department of Veterinary Anatomy and Histology, Mumbai Veterinary College, Mumbai and underwent computed tomographic (CT) imaging of liver at Chitra Scan Centre, Dadar, Mumbai. Non-contrast CT scanning was carried out using a 128 slice computed tomographic scanner by Optima 660 (GE healthcare). Imaging parameters included a tube voltage of 120-140 kVp, tube current of 100-160 mA, slice thickness of 0.6 mm, and reconstruction interval of 0.3 mm using soft tissue window settings (window width 350 HU; window level 40 HU). Additional scan parameters were set at pitch 1, tube rotation 0.5-1 sec.

For the purpose of computed tomographic scan, each cadaver was positioned in right lateral recumbency on the CT table, with limbs extended to ensure consistent positioning across specimens (Fig. 1). The area of interest for this study extended from the caudal thoracic region, approximately at the level of the eighth thoracic vertebra (T8) to the cranial lumbar region, approximately up to the level of the fourth lumbar vertebra (L4) to ensure complete visualization of the cranial abdominal organs. Multiplanar reconstructions in the sagittal, transverse and dorsal plane images were generated to facilitate detailed assessment of organ orientation, craniocaudal extent, and spatial relationships, as well as correlation with vertebral levels. Transverse images constituted the primary dataset for anatomical evaluation. Image analysis was performed on a dedicated workstation using software DICOM Viewer. Organ position, shape, margins, surface contours, parenchymal attenuation and relationships with adjacent structures were assessed. Because of differences in body size from one animal to another, vertebrae were used as reference landmarks to explain the position of abdominal structures as stated by Shojaei *et al.* (2006) in cats. Attenuation values were measured in Hounsfield units (HU) within representative areas of each organ while avoiding peripheral margins and interfaces.

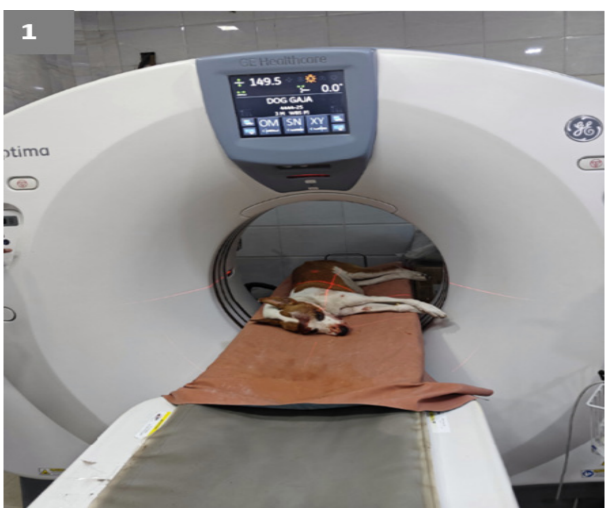

Fig. 1: Multislice computed tomographic (CT) system (Optima 660- GE healthcare) and the dog cadaver undergoing computed tomography in the right lateral recumbency.

Results and Discussion

Helical transverse computed tomographic images were evaluated to establish the typical location, shape, extent, and attenuation characteristics of liver with special emphasis on vertebral level-wise visualization in dog cadavers. Sagittal and dorsal plane images were also obtained to study the relationship of liver with other organs. Computed tomographic images in this study were orientated so that the left side of the abdominal cavity was to the viewer's left and dorsal was at the top (Fig. 3-7). The computed tomographic image of the dog cadaver with vertical lines represented the approximate level of each transverse plane image in the thoracic and abdominal regions (Fig. 2). The topographical positions of the liver according to thoracic (T) and lumbar (L) vertebrae in dog cadaver ranged from T8 to L1. The mean values of Hounsfield units (HU) for the liver were 68.68 ± 5.48 (range 54.2-89.0), and for gall bladder 58.51 ± 5.03 (range 38.5-71.0).

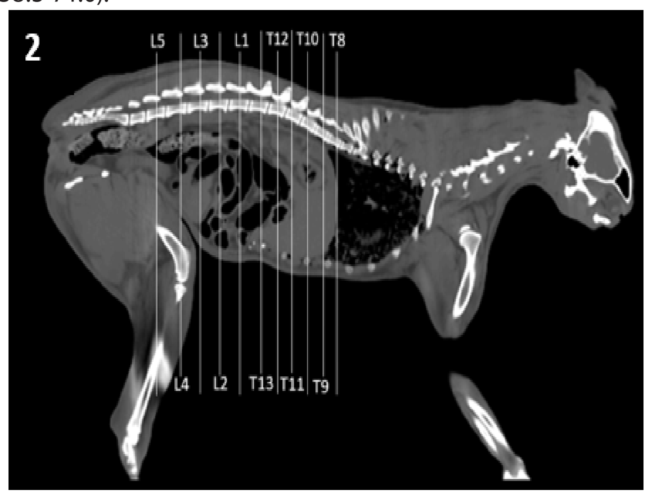

Fig. 2: CT image of adult dog cadaver with vertical lines representing the approximate level of each transverse plane in the thoracic and abdominal regions shown in Fig. 3-7.

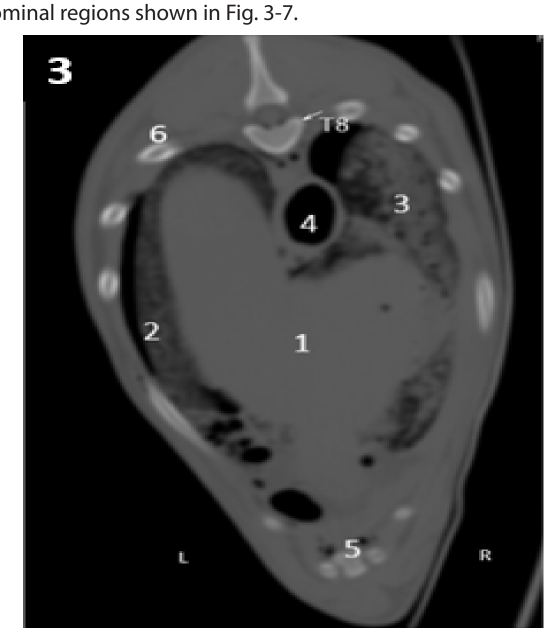

Fig. 3: Transverse CT image of cranial abdomen at the level of eighth thoracic vertebra. 1. Liver, 2. Left lung, 3. Right lung, 4. Oesophagus, 5. Sternum, 6. Rib, T8- 8th thoracic vertebra.

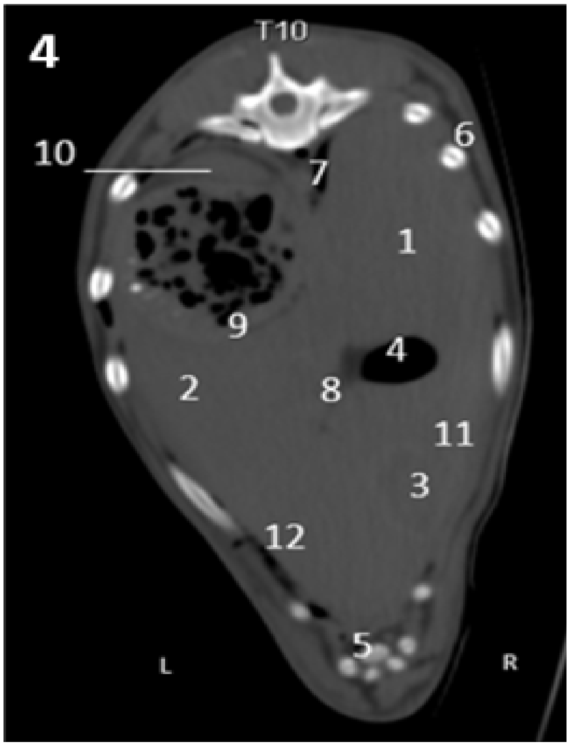

Fig. 4: Transverse CT image of cranial abdomen at the level of tenth thoracic vertebra. 1. Right lateral lobe of liver, 2. Left lateral lobe of liver, 3. Gall bladder, 4. Intestinal loop, 5. Sternum, 6. Rib, 7. Right lung, 8. Falciform ligament, 9. Fundus of the stomach, 10. Splenic head, 11. Right central liver lobe, 12. Left central liver lobe, T10- 10th thoracic vertebra.

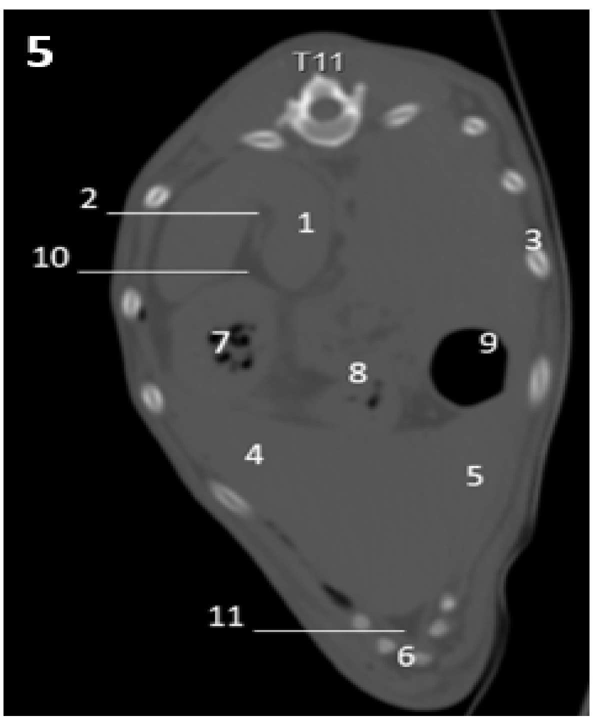

Fig. 5: Transverse CT image of cranial abdomen at the level of eleventh thoracic vertebra. 1. Spleen, 2. Splenic hilus, 3. Rib, 4. Left lateral lobe of liver, 5. Right lateral lobe of liver, 6. Sternum, 7, 8. Body of the stomach, 9. Intestinal loop, 10. Greater omentum, 11. Falciform ligament, T11- 11th thoracic vertebra.

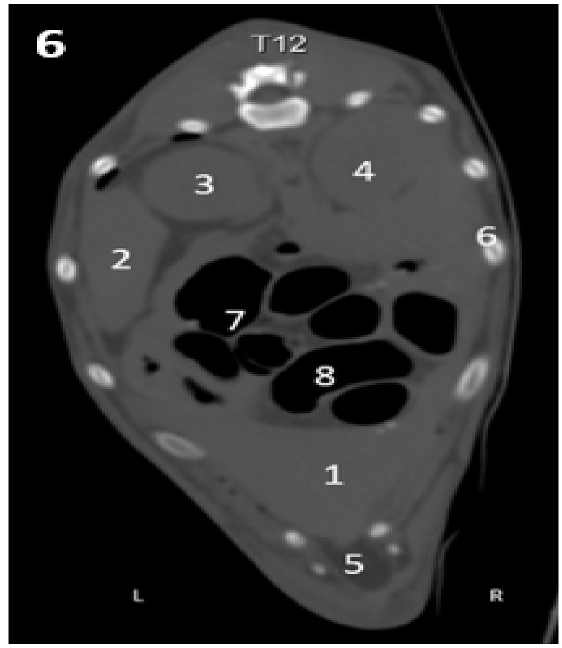

Fig. 6: Transverse CT image of cranial abdomen at the level of twelfth thoracic vertebra. 1. Liver, 2. Spleen, 3. Left kidney, 4. Right kidney, 5. Falciform ligament, 6. Rib, 7,8. Intestinal loops, T12- 12th thoracic vertebra.

Computed Tomography of the Liver in Dog Cadaver

On non-contrast computed tomography, the liver was consistently identified as a homogeneous parenchymatous organ in soft tissue density, occupying the cranial abdominal cavity. The hepatic parenchyma appeared to be continuous with the diaphragm. Similar observations were reported by Schwarz and Saunders (2011) in dogs. Rivero *et al.* (2009) reported that the liver was of intermediate computed tomographic density, whereas Alsafy *et al.* (2022) mentioned that it was moderate density in Baladi dog cadavers. No focal hyper or hypodense areas were observed. The mean attenuation value of liver recorded in the present study was 68.68 ± 5.48 HU (range was 54.2-89.0 HU), which may indicate soft tissue density. Minor alteration in the tissue density of liver observed may be due to embalming of dog cadaver. Schwarz and Saunders (2011) stated that the density of the liver was 60-70 HU in dogs and 42-65 HU in cats. The liver was hyperattenuating to the muscle and hypoattenuating to the bony structures of the ribs, vertebrae or sternum. The liver was hyperattenuating than the falciform ligament, mesentery and the perirenal fat (Fig. 4, 7). Rivero *et al.* (2009) noted that the CT images provided a good differentiation of the soft tissues from the bone. The liver extended from the cranial abdominal region into the lumbar region. It became visible between T8 and T9 and tapered caudally by T13-L1 vertebra (Fig. 3-7). The caudal extent of the liver varied slightly among individuals but did not extend beyond the level of the first lumbar vertebra. Similar observations were reported in CT evaluations of liver by Alsafy *et al.* (2022) in

Baladi dog cadavers and Al-Akraa *et al.* (2015) and Shojaei *et al.* (2006) in cats. On computed tomographic images, compact appearance of the liver was observed with indistinct hepatic lobes. This observation was in accordance with the findings of Schwarz and Saunders (2011) in dog, who reported that the various anatomical regions become more enhanced in post-contrast computed tomography. Lobar differentiation has been reported by Teixeira *et al.* (2007) and Rivero *et al.* (2009) in dogs and Al-Akraa *et al.* (2015) in cats. The cranial surface of the liver conformed to the diaphragmatic curvature and its caudal surface was directed toward the stomach, spleen, right kidney and proximal intestinal tract (Fig. 8-9). Similar observations were reported by Nishi *et al.* (2024) in dogs and Al-Akraa *et al.* (2015) in cats.

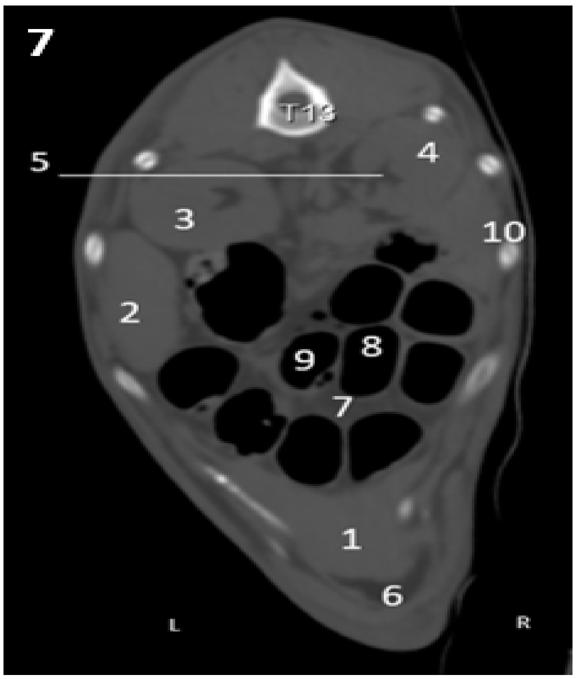

Fig. 7: Transverse CT image of cranial abdomen at the level of thirteenth thoracic vertebra. 1. Liver, 2. Spleen, 3. Left kidney, 4. Right kidney, 5. Fatty renal hilus of the right kidney, 6. Falciform ligament, 7. Mesentery, 8,9. Intestinal loops, 10. Rib, T13- 13th thoracic vertebra.

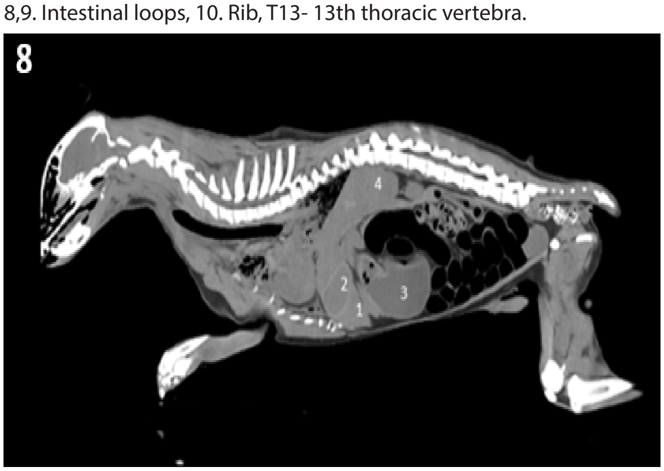

Fig. 8: Parasagittal CT image of the thorax and abdomen. 1. Liver, 2. Gall bladder, 3. Stomach, 4. Spleen.

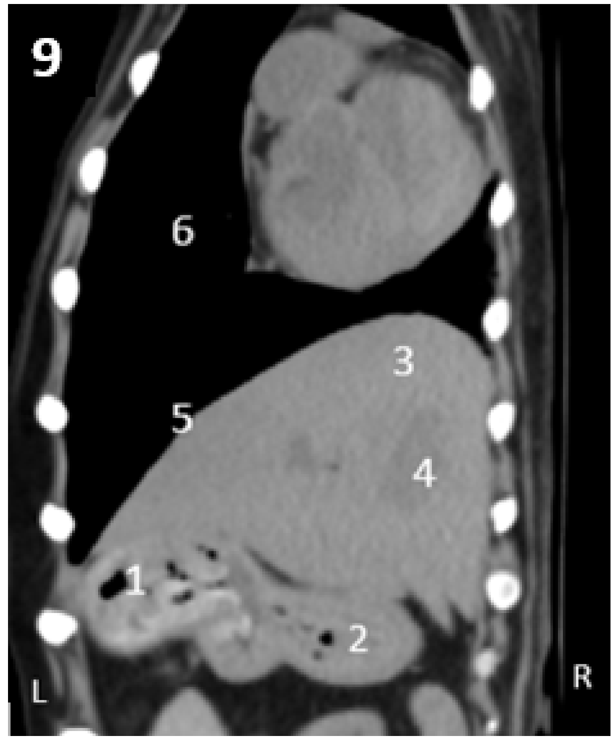

Fig. 9: Dorsal CT image of the thorax and cranial abdomen. 1. Fundus of the stomach, 2. Body of the stomach, 3. Liver, 4. Gall bladder, 5. Diaphragm, 6. Left lung.

A. Transverse Plane

In transverse computed tomographic images, the hepatic tissue became visible as a small homogenous structure, followed by progressive enlargement to maximal cross-sectional area between T9 and T10 and subsequent tapering caudally.

At the level of the eighth thoracic vertebra, the appearance of the liver parenchyma observed in the present study corresponds with the cranial extent of the canine liver in non-contrast computed tomographic examinations. Alsafy *et al.* (2022) observed a similar appearance at the T10 level in Baladi dog cadavers; this could be because of the larger dogs used in their study. Samii *et al.* (1998) and Al-Akraa *et al.* (2015) also observed similar appearance of the liver in cats. The presence of aerated caudal lung lobes adjacent to the hepatic tissue, appeared as markedly hypoattenuating regions at this level. The caudal lobes of the lungs appeared black with a low computed tomographic density compared to hepatic parenchyma of a soft tissue. These observations are in accordance with the findings of Rivero *et al.* (2009) in cranial abdomen of dogs. Similar appearance of lung lobes around the liver was also reported by Al-Akraa *et al.* (2015) in cats. The oesophagus was observed as a circular structure dorsal to the liver (Fig. 3). This is in accordance with the findings reported by Schwarz and Saunders (2011) in dogs. Similar observation has also been documented in transverse CT images by Alsafy *et al.* (2022) in Baladi dog cadavers and Shojaei *et al.* (2006) in cats.

At the level of the ninth thoracic vertebra, the liver occupied a substantial portion of the abdominal cross-section. Similar observation was noted by Rivero *et al.* (2009) in dogs. The left lobes of the liver overlapped with the stomach fundus at this level on the left side of the median plane. Similar relationship of liver with the stomach was observed by Rojo *et al*. (2020) in cats and Schwarz and Saunders (2011) in dogs. The gall bladder was identified towards the left of the homogenous right central hepatic lobe. The wall of the gall bladder was not clearly visible. Similar findings were reported by Schwarz and Saunders (2011) in dogs. The gall bladder was a slightly hypoattenuated pear-shaped structure within the hepatic parenchyma at this level. Similar observation was also noted by Rojo *et al*. (2020) in cats. Rivero *et al*. (2009) also reported that the contour of the gall bladder could be discerned on the hepatic parenchyma in dogs.

At the tenth thoracic vertebral level, the liver occupied most of the area in transverse cross-section (Fig. 4). Alsafy *et al*. (2022) observed similar findings at the level of T11 vertebra in Baladi dog cadavers. This may be because of larger body conformation of dogs used in their study or due to breed variation. The margins were smooth and the liver parenchyma appeared as a homogenous soft tissue. The falciform ligament and the gall bladder appeared darker than the hepatic parenchyma. A hypoattenuated region near the gall bladder showed presence of falciform ligament (Fig. 5, 6). The stomach was located close to the caudal hepatic margin and the stomach wall was distinctly visualised.

At the eleventh thoracic vertebra, a gradual reduction in hepatic cross-sectional area was observed, marking the transition toward the caudal hepatic margin (Fig. 5). The body of the stomach was placed adjacent to the left lateral lobe of the liver. The homogeneous hepatic parenchyma with soft tissue density had smooth margins and appeared to be of similar density as the spleen. Similar observations have been reported by Alsafy *et al.* (2022) in Baladi dog cadavers, Rivero *et al*. (2009) in dogs and Rojo *et al*. (2020) in cats. Rivero *et al.* (2009) stated that the greater omentum appeared dark grey with lower computed tomographic density as compared to the liver due to presence of adipose tissue.

At the twelfth thoracic vertebral level, the caudal-most portions of the liver were visualized as tapering structures ventrally (Fig. 6). The falciform ligament was visualised as a hypodense area ventral to the hepatic parenchyma (Fig. 5-7). Similar observation was reported by Schwarz and Saunders (2011) in dogs. The simultaneous visualization of both kidneys ventrolateral to the vertebral column was observed in this image. The liver, spleen and kidneys appeared slightly grey with a homogenous soft tissue density. Rivero *et al.* (2009) noted that liver and right kidney were in intermediate density in dogs.

Beyond the twelfth thoracic vertebra, the liver was minimally visible, marking its caudal anatomical extent (Fig. 7). Al-Akraa *et al.* (2015) observed the presence of liver at the level of the L1 vertebra in cats. Rivero *et al.* (2009) observed the caudal extent of liver between the T13 and L1 vertebra in dogs. Cha *et al.* (2018) identified the caudal border of the liver at cranial L2 vertebra in sagittal reconstruction in Beagle dogs. This difference could be attributed to non-descript breed of dogs used in the present study. Cha *et al*. (2018) also mentioned that greater caudal extension of liver was visible on dogs with shallow and wide thoracic conformation whereas in deep chested dogs, the liver lay more completely within the costal arch.

B. Sagittal and Dorsal Plane

In the present study, sagittal computed tomographic image demonstrated the convex parietal surface and mildly concave visceral surface of the liver (Fig. 8). The parietal surface of the liver was related to the diaphragm. The visceral surface of the liver showed close association with adjacent cranial abdominal organs. Similar appearance of the liver was reported by Alsafy *et al.* (2022) in Baladi dog cadavers and Cha *et al*. (2018) in Beagle dogs. Dorsal reconstruction provided an understanding of the location of the hepatic parenchyma. It occupied a substantial portion of the cranial abdomen (Fig. 9). Similar observation was reported by Schwarz and Saunders (2011) in dogs. It was observed that the hepatic tissue had a right-sided predominance and extended across the midline. The fundus and body of the stomach was observed adjacent to the caudal hepatic border. The gall bladder was slightly hypoattenuated as compared to the hepatic parenchyma.

Conclusion

In the present study, helical non-contrast computed tomography was observed to be an effective cross-sectional imaging modality for the assessment of morphology and anatomical relationships of liver with surrounding organs in embalmed dog cadavers.

Acknowledgement

The authors are grateful to the Associate Dean, Mumbai Veterinary College for providing necessary infrastructural facilities and financial grants to carry out the research work. The authors are also thankful to Dr. Rajesh Asnani, Director, Chitra Scan Centre for his valuable guidance.

References

Al-Akraa, A.M., Ghanem, M.M., & El-gezery, M.M. (2015). Hepatosonography and computed tomography in feline. *Benha Veterinary Medical Journal, 28*(1), 33-42.

Alsafy, M.A.M., Hanafy, B.G., Rutland, C.S., Karkoura, A.A., Enany, E.S., & El-Gendy, S.A.A. (2022). Morphological investigation of canine epigastric organs and adjacent structures via computed tomography, ultrasound and anatomical prosection. *Morphologie, 106*(355), 271-286.

Cha, A., Park, S., Kim, C., Yoon, S., Lee, D., Kim, D., Chang, D.W., & Choi, J. (2018). Effect of radiographic technique on assessment of liver size in Beagles. *American Journal of Veterinary Research, 79*(11), 1133-1139.

Gavrilas, E., Miró, F., Blanco, B., Lucena, R., Ginel, P.J., & Novales, M. (2016). Helical computed tomography – anatomy of the cat abdomen. *Bulletin of University of Agricultural Sciences and Veterinary Medicine, 73*(1), 149-152.

Hoey, S., Randi, D., & Scott, H. (2012). Evaluation of the gastrointestinal tract in dogs using computed tomography. *Veterinary Radiology and Ultrasound*, *54*(1), 1-6.

Mannion, P. (2006). The liver and spleen. In: *Diagnostic Ultrasound in Small Animal Practice*. Mannion, P., Oxford: Blackwell Science, Chapter 5, p. 50-70.

Nishi, R., Moore, G., & Murakami, M. (2024). A reference interval for CT-based liver volume in dogs without hepatic disease. *Veterinary Sciences, 11*(9), 400.

Rivero, M.A, Va´zquez, J.M., Gil, F., Ramı´rez, J.A., Vilar, J.M., De Miguel, A., & Arencibia, A. (2009). CT-soft tissue window of the cranial abdomen in clinically normal dogs: An anatomical description using macroscopic cross-sections with vascular injection. *Anatomy, Histology & Embryology, 38,* 18-22

Rojo, D., Vázquez, J.M., Sánchez, C., Arencibia, A., García, M.I., Soler, M., Kilroy, D., & Ramírez, G. (2020). Sectional anatomic and tomographic study of the feline abdominal cavity for obtaining a three-dimensional vascular model. *Indian Journal of Veterinary Research, 21*(4), 279-286.

Samii, V.F., Biller, D.S., & Koblik, P.D. (1998). Normal cross-sectional anatomy of the feline thorax and abdomen: comparison of computed tomography and cadaver anatomy. *Veterinary Radiology & Ultrasound,39*(6), 504-511.

Schwarz, T., & Saunders, J. (2011). *Veterinary Computed Tomography.* Chichester, West Sussex, UK: Wiley-Blackwell

Shojaei, B., Vajhi, A.R., Rostami, A., Molaei, M.M., Arashian I., & Hashemnia, S. (2006). Computed tomographic anatomy of the abdominal region of cat. *Iranian Journal of Veterinary Research, University of Shiraz, 7*(2), 45-52.

Teixeira, M., Gil, F., Vazquez, J.M., Cardoso, L., Arencibia, A., Zarzosa, G.R., & Agut, A. (2007). Helical computed tomographic anatomy of the canine abdomen. *The Veterinary Journal, 174*, 133-138.

ANNOUNCEMENT - II
BEST PAPER AWARDS: SVSBT-2026

Applications in the prescribed format are invited from the **Life Members** of the Society for the **SVSBT Awards - 2026** for the **Best Research Papers (I & II) and the Best Clinical Case Report (I) published in IJVSBT, Vol. 21**, **Issue Nos. 1 to 6 (January to December 2025).** The awards will be honoured to the deserving scientists during the inaugural ceremony of ***XIII Annual Convention*** and ***National Conference of SVSBT*** to be held **during October 6-7, 2026** at College of Veterinary Sciences, **BASU, Patna-800014,** Bihar, India.

The interested LMs can apply in the prescribed format given below. The **application (scanned copy) along with a PDF copy of Published article** must be submitted online on or before **31st July, 2026 to the President, SVSBT, Anand**, **Gujarat at e-mail: ajdhami59@gmail.com.** It is **mandatory that all authors of the paper under contest should be life members of the Society**. Applications received incomplete and/or after the due date will not be entertained.

APPLICATION FORM for SVSBT BEST PAPER AWARDS

1.	**Title of the Research Paper / Case Report:**			
2.	**IJVSBT 2025 :**	**Vol.: 21**	**Issue No.: ....**	**Pages: ....**
3.	**Authors' detail :** (Plz add in sequence)	**Sr. No.**	**Name**	**LM No.**
		1		
		2		
		3		
		4		
		5		
		6		
4.	Main Corresponding author for Award:	Name:	Contact No.:	E-mail:
5.	Postal address with PIN code:			
6.	Did you receive this award earlier? If yes, plz give year.			
Date: Place:				Signature with date & name of applicant